Global and Planetary Change 198 (2021) 103406

Contents lists available at ScienceDirect

Global and Planetary Change

journal homepage: www.elsevier.com/locate/gloplacha

Tree growth decline as a response to projected climate change in the 21st century in Mediterranean mountain forests of Chile

Vladimir Matskovsky [a,1], Alejandro Venegas-González [b,*,1], René Garreaud [c,d], Fidel A. Roig [e,b], Alvaro G. Gutiérrez [f], Ariel A. Muñoz [d,g], Carlos Le Quesne [h], Karin Klock [g], Camila Canales [f]

[a] Institute of Geography RAS, Moscow, Russia
[b] Hémera Centro de Observación de la Tierra, Escuela de Ingeniería Forestal, Facultad de Ciencias, Universidad Mayor, Santiago, Chile
[c] Departamento de Geofísica, Universidad de Chile, Santiago, Chile
[d] Center for Climate and Resilience Research, Santiago, Chile
[e] Laboratorio de Dendrocronología e Historia Ambiental, IANIGLA-CONICET-Universidad Nacional de Cuyo, Mendoza, Argentina
[f] Departamento de Ciencias Ambientales y Recursos Naturales Renovables, Universidad de Chile, Santiago, Chile
[g] Instituto de Geografía, Pontificia Universidad Católica de Valparaíso, Valparaíso, Chile
[h] Laboratorio de Dendrocronología y Cambio Global, Facultad de Ciencias Forestales y Recursos Naturales, Universidad Austral de Chile, Valdivia, Chile

ARTICLE INFO

Keywords:
Austrocedrus chilensis
Climate change
Climatic projections
Dendroecology
Nothofagus macrocarpa
Tree rings
South American Mediterranean forest
Vaganov–Shashkin-Lite model

ABSTRACT

Global Climate Models project that observed climate trends are likely to be preserved and the number of extreme events will be increasing during the rest of the 21st century, which may have a detrimental impact on forest ecosystems. These impacts may include forest decline and widespread dieback of the most vulnerable biomes, such as the Mediterranean Forest of Central Chile (MFCC). *Nothofagus macrocarpa* and *Austrocedrus chilensis* are two canopy-dominant, endangered tree species in the mountains of MFCC. Here, we project tree growth of these species based on tree-ring width chronologies, a simplified version of a process-based model, and climate change projections. We used the tree ring information derived from ~400 trees from 12 sites distributed across MFCC in combination with the simplified version of process-based Vaganov-Shashkin tree-growth model (VS-Lite) to forecast changes in tree growth for the next four decades. Tree growth projections were made on the basis of monthly values of temperature and precipitation from the output of 35 climate models based on two ensembles of CO_2 emission scenarios of the IPCC AR5 (RCP 8.5: higher-emission scenario, and RCP 2.6: lower-emission scenario). For the MFCC region these scenarios result in temperature rise ranging between 0.5 °C and 2.0 °C, and a precipitation decrease between 5% and 20% by the year 2065, as related to historical conditions. Our results showed that the VS-Lite model is capable of reproducing tree growth decline during the recent extreme dry period, i.e. 2010–2018, which supports its use for tree growth projections in the MFCC region. According to the modeling results, we find that tree growth in both *N. macrocarpa* and *A. chilensis* forests distributed in the MFCC region will be adversely affected by future climate changes, mainly starting from the year 2035, under both scenarios. Our work provides evidence of the degree of vulnerability of Mediterranean mountain forests in central Chile according to current climate change projections. The projected decline in tree growth indicates serious risks in the dynamics and survival of these forests relatively soon, so alerts are given about this situation which may require to counteract the deleterious effects of global change on vegetation in this region.

1. Introduction

There is ample evidence that global warming has intensified during the last decades, and drought episodes have been more severe (Jones et al., 2001; O'Neill et al., 2017). Under scenarios of increased greenhouse gases emissions (GHG), Global Climate Models (GCMs) project an increase in these trends and episodes by the end of the 21st century (Pachauri et al., 2014), particularly in Mediterranean regions of the world (Giorgi and Lionello, 2008). Pronounced drought conditions triggered by climate change directly affect forest ecosystems, resulting

* Corresponding author at: Camino La Pirámide 5750, Huechuraba, Santiago, Chile.
E-mail address: alejandro.venegas@umayor.cl (A. Venegas-González).
[1] Equal contribution to the work.

https://doi.org/10.1016/j.gloplacha.2020.103406
Received 6 November 2019; Received in revised form 14 December 2020; Accepted 22 December 2020
Available online 26 December 2020

in forest decline and widespread dieback in different biomes worldwide (Allen et al., 2010, 2015; Anderegg et al., 2015).

The Mediterranean forest of Central Chile (hereafter MFCC, Fig. 1), the only mediterranean-type ecosystem of South America, is currently under a state of strong vulnerability due to forest fragmentation produced by logging and land use change (Miranda et al., 2016), wildfires, and climate change (Bowman et al., 2019; González-Reyes et al., 2017). The MFCC ecosystem still dwells a high biodiversity of endemic species, being declared a global biodiversity hotspot (Armesto et al., 2007; Myers et al., 2000). The MFCC ecosystem is a host of the two tree species that reach the northernmost distribution of their genus in this region: the broadleaf *Nothofagus macrocarpa* [(DC.) Vásquez and Rodr.] and the conifer *Austrocedrus chilensis* [(D. Don) Pic. Ser et Bizz.]. Both tree species represent relict forests from the last glacial period (Villagrán, 1995), share a similar macroclimate setting (Arroyo et al., 1993), and are presently considered endangered (Baldwin, 2018; Souto and Gardner, 2013). Moreover, these trees have been signaled as highly-valuable sources for palaeoclimatic research (Boninsegna et al., 2009; Le Quesne et al., 2006; Oliveira et al., 2010; Roig et al., 2006; Venegas-González et al., 2018a, b; Villalba and Veblen, 1998), which constitutes a relevant factor for this study due to the significant sensitivity of their ring widths to climatic variability.

During the last three decades MFCC have been influenced by a marked drying (Boisier et al., 2018, 2016) and a sustained warming trend (Burger et al., 2018; Vuille et al., 2015), phenomena that significantly impacted the radial growth of *N. macrocarpa* and *A. chilensis* (Garreaud et al., 2017; Le Quesne et al., 2006; Venegas-González et al., 2018b). An uninterrupted sequence of dry years has been observed in central Chile since 2010, partially forced by repeated neutral El Niño Southern Oscillation (ENSO) conditions, causing annual rainfall deficits in the range of 25–45% (Garreaud et al., 2017, 2020). Drought has had a significant effect on the Mediterranean ecosystems of central Chile with increased number of large wildfires and prolonged fire season among other consequences (González et al., 2018). According to a dendroclimatic drought reconstruction (Muñoz et al., 2020), the current drought that has affected the MFCC region represents an unprecedented phenomenon in the past six centuries.

GCMs project that the observed drying/warming trends will continue in the future (O'Neill et al., 2017). Annual temperature increase from ~1.2 °C (RCP 2.6) to ~3.5 °C (RCP 8.5), and drying from ~3% (RCP 2.6) to ~30% (RCP 8.5) by the year 2100 is expected in MFCC, based on scenarios from different Representative Concentration Pathways (RCPs) with a wide range of possible changes in future anthropogenic GHG emissions (Bozkurt et al., 2018). According to recent studies, anthropogenic forcing appears to be the leading factor driving the temperature increase and reduction in precipitation and runoff in the MFCC region (Barria et al., 2019; Boisier et al., 2018; Muñoz et al., 2020). However, the response of MFCC to the projected climate change is not well studied yet.

So far, several approaches for projecting tree growth into the future have been used (Chen et al., 2010; Guiot et al., 2014; Charney et al., 2016; Gea-Izquierdo et al., 2017; Pompa-García et al., 2017; Sánchez-Salguero et al., 2017a, 2017b; Rahman et al., 2018; etc.) such as: linear approach (e.g. Chen et al., 2010; Pompa-García et al., 2017; Sánchez-Salguero et al., 2017a, 2017b; Rahman et al., 2018), process-based approach (e.g. Guiot et al., 2014; Gea-Izquierdo et al., 2017), and empirical approach (e.g. Charney et al., 2016). However, each of these approaches has advantages and limitations. The main limitation of the linear approach is that it may violate one of the basic principles of tree growth - the principle of limiting factors. This principle (initially defined by Liebig in 1840) states that the rate of plant growth is constrained by the environmental resource which is in the least supply at each moment of tree growth (Fritts, 1976). Applied to tree-growth projections it means that, for instance, given an increasing temperature but constant moisture supply, at a certain point temperature may stop being the limiting factor while soil moisture will start to limit tree growth when less water is reaching plant roots due to increased evaporation, i.e. a non-stationary response (Wilmking et al., 2020). In the case of the linear

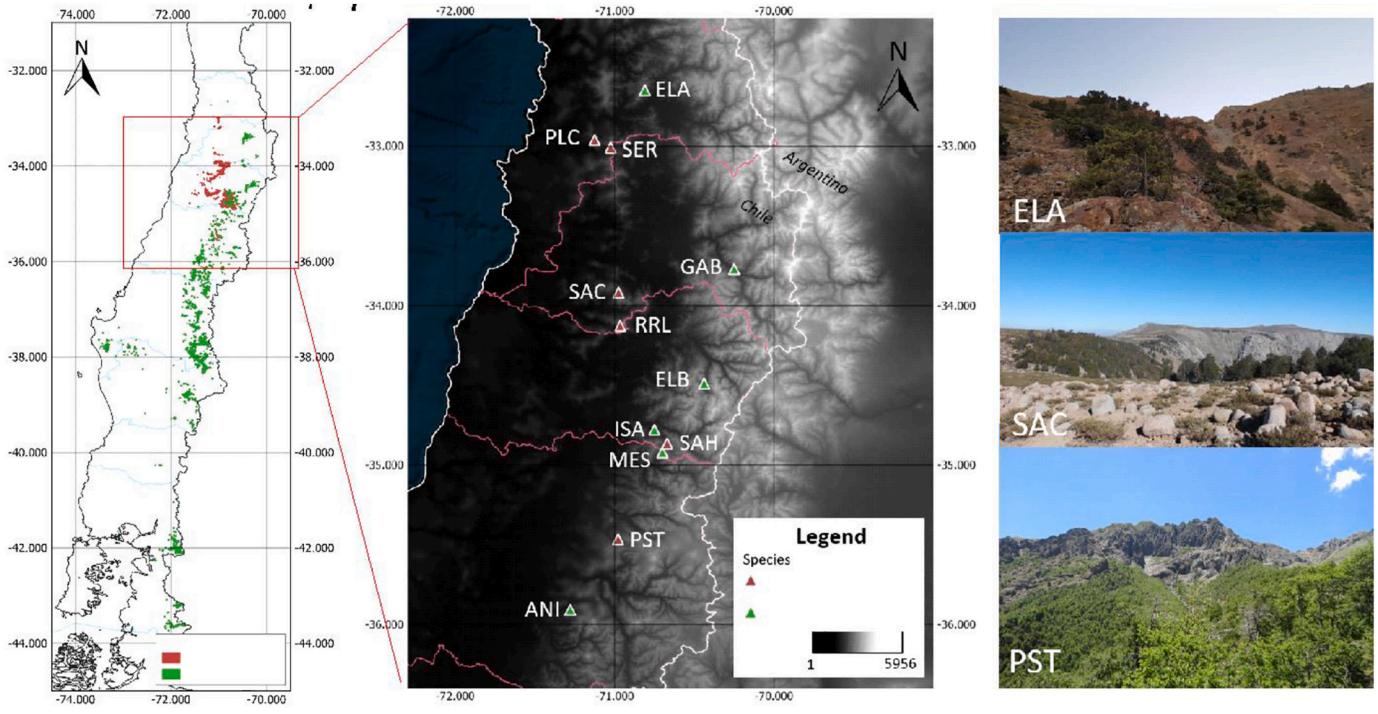

Fig. 1. Left figure shows the natural distribution of the studied tree species. Figure at the center shows the study forest stands of *N. macrocarpa* (red triangles) and *A. chilensis* (green triangles) in MFCC. Right figures show certain sampled tree populations (from top to bottom: *A. chilensis* population in El Asiento (ELA), *N. macrocarpa* in Nature Sanctuary Altos de Cantillana (SAC), and *N. macrocarpa* in National Park Siete Tazas (PST). (For interpretation of the references to colour in this figure legend, the reader is referred to the web version of this article.)

approach it means that some of the climatic parameters in the linear equation can change their coefficients and even signs, so that the initial prognostic equation will not be valid. In this sense, process-based models of tree-ring formation provide a more physiologically-based approach for studying growth response to future climate variability, as compared to linear models. Such models can represent mixed and non-linear tree growth responses to changing climatic factors, thus implementing the principle of limiting factors. They also may take into account different types of processes involved into tree growth (see Table 1 in Guiot et al., 2014), thus better representing tree physiology.

One of the most explicit process-based forward models of tree growth is the Vaganov-Shashkin (VS) model (Vaganov et al., 2011). Since this model is rather sophisticated in application, having more than 40 tunable parameters and daily resolution, it has been adapted for more practical application using monthly resolution with fewer tunable parameters. The VS-Lite model (Tolwinski-Ward et al., 2011) is perhaps the best available model for studying the nature of non-linear tree growth response in regions where daily climate data and field observations are not readily available or limited (Lavergne et al., 2015). Here we used the VS-Lite model for tree growth projections under different GHG emissions scenarios (RCP 2.6 – increase and decline emissions scenario and RCP 8.5 – heavy emissions scenario) calculated for central Chile, using output of regional, continental-scale and global climate models, and tree-ring chronologies of the two highly endangered tree species of MFCC: *N. macrocarpa* and *A. chilensis*. Following its application for modeling a global network of tree-ring chronologies (Breitenmoser et al., 2014), VS-Lite model has become increasingly popular for tree growth modeling in different forest ecosystems (e.g. Björklund et al., 2019; Matskovsky et al., 2019; Zeng et al., 2019) due to its ability to jointly account for temperature and precipitation as the main climatic factors affecting tree growth and due to its relative simplicity.

The specific objectives for this study were: (i) to calibrate and validate the VS-Lite model based on a newly developed network of tree-ring chronologies for *N. macrocarpa* and *A. chilensis* from MFCC and (ii) to obtain tree-growth projection for these two species under two projected climatic scenarios (RCP 2.6 and 8.5) for the period 2005–2065. We hypothesize that the heavy emissions scenario (RCP 8.5) will result in significant regional forest decline by the end of the 21st century, while the scenario of lower emissions (RCP 2.6) will slow down this process in the future decades. We expect that this assessment will improve our knowledge of MFCC forests vulnerability to climate change, especially for the two endemic tree species selected, providing certain assistance in developing targeted conservation strategies for the MFCC woodlands.

2. Materials and methods

2.1. Study areas and selected tree species

The study area is located in the main distribution of MFCC between 32°57′ and 35°54′S, and between 71°07′ and 70°15′W (Fig. 1), with typical Mediterranean climate characterized by a rainy winter (June to August) and a prolonged dry season lasting from early spring to early autumn (October to April). Because of the orographic precipitation enhancement, annual mean rainfall varies from about 300 mm in the lowland coastal sector to about 1500 mm in the higher terrains of the Andes cordillera (Table S1, Viale and Garreaud, 2015). The inter-annual variation in rainfall is high and strongly influenced by El Niño Southern Oscillation (ENSO), with warm (cold) events in central equatorial Pacific often associated with wet (dry) conditions in central Chile (Montecinos and Aceituno, 2003). Along the Andean range, soils were developed on volcanic or granitic rocks and from glacial sediments, they are classified as brown soils, and vary from medium-deep on slopes to deep in high plains (Villagrán, 1995). Along the Coastal range, soils were formed from granitic rocks and poorly developed, usually residual on rocky outcrops (Donoso, 1982).

N. macrocarpa trees ("Roble de Santiago", Nothofagaceae) and *A. chilensis* ("Ciprés de la Cordillera", Cupressaceae), are two endangered long-lived tree species growing at high altitudes (>1200 m a.s.l.) whose natural distribution extends in the mountains of MFCC (Luebert and Pliscoff, 2006). *N. macrocarpa* is a deciduous tree species, reaching 25 m of height and > 60 cm of stem diameter at breast height (Gajardo, 2001), endemic to the Chilean Mediterranean region. The structure of these forests usually includes a high arboreal stratum of scattered old individuals, the remnants of previous stand structures that were probably intervened by fire or logging. In situations with low canopy cover, it is possible to distinguish a sclerophyllous shrub stratus (1–2 m), highly variable in density and in species composition according to the altitudinal range (~ 1000 m a.s.l.). *Austrocedrus chilensis* is a tree species whose northern natural limit of distribution reaches MFCC (Castor et al., 1996), forming open and sparsely distributed stands (Cruz, 2015) and representing the driest conditions in which this species survives along its distribution (Schlegel, 1962).

2.2. Tree-ring chronologies

We selected 12 sites (six per each tree species) distributed along a latitudinal gradient in MFCC in both mountain systems, the Coastal and the Andes ranges. For *N. macrocarpa*, between April 2014 and December 2017, we sampled four sites in the Coastal range and two sites in the Andean Cordillera, for what was possible to include populations representing the entire species' distribution (Fig. 1, Table 1). At each of these

Table 1
Main characteristics of the tree-ring chronologies. Dbh: diameter at breast height. Number of trees and radii per site. Tree-ring width (TRW, mm) was determined from cores taken at 1.3 m. Rbar: is the mean correlation coefficient for all possible pairings among tree-ring series from individual cores, computed for a specific common time interval. MS: is the mean sensitivity considering the time span (TS).

Species	Site (Code)	N°trees/radii	TRW ± D	RBar	MS	TS (years)
N. macrocarpa	La Campana (PLC)	29/47	1.34 ± 0.88	0.35	0.45	1929–2014
N. macrocarpa	El Roble (SER)	29/42	1.81 ± 1.17	0.37	0.50	1921–2014
N. macrocarpa	Altos de Cantillana (SAC)	24/46	1.39 ± 0.78	0.21	0.47	1826–2014
N. macrocarpa	Robleria de Loncha (RRL)	23/37	1.69 ± 0.90	0.25	0.40	1890–2014
N. macrocarpa	Alto Huemul (SAH)	41/56	1.39 ± 0.73	0.26	0.39	1832–2014
N. macrocarpa	Parque 7 Tazas (PST)	35/61	1.37 ± 0.75	0.25	0.39	1849–2016
A. chilensis	El Asiento (ELA)	54/105	0.64 ± 0.36	0.27	0.30	884–2017
A. chilensis	San Gabriel (GAB)	40/65	0.44 ± 0.25	0.40	0.26	1131–1975
A. chilensis	El Baule (ELB)	46/72	0.58 ± 0.31	0.45	0.25	1540–2011
A. chilensis	Santa Isabel (ISA)	40/77	0.65 ± 0.41	0.44	0.21	1568–1975
A. chilensis	Alto de las Mesas (MES)	19/19	1.99 ± 0.97	0.53	0.24	1796–1975
A. chilensis	Las Animas (ANI)	18/34	1.89 ± 0.93	0.23	0.26	1879–2017
N. macrocarpa	**Regional**	**181/350**	**1.64 ± 0.91**	**0.19**	**0.43**	**1826–2016**
A. chilensis	**Regional**	**217/372**	**0.80 ± 0.42**	**0.27**	**0.26**	**884–2017**

sites, we sampled ~30 living trees in an area of ~1.0 ha (2–4 cores per tree), selecting random individuals of different sizes. Wood cores were extracted from single-stemmed living trees and from trunk portions without cracks, fire scars or other anomalies that could create difficulties at the ring width distinction and measurement stage. All tree-ring samples were stored at the wood collections of different dendrochronological laboratories in Chile (in Santiago, Valparaíso and Valdivia). In the case of *A. chilensis,* the tree-ring width data were downloaded from the International Tree Ring Data Bank (ITRDB, https://www.ncdc.noaa.gov/data-access/paleoclimatology-data/datasets/tree-ring). These data ended in the 1970s, therefore, we both updated the chronologies up to the year 2017 with samples acquired in several campaigns during the last decade and expanded the network of chronologies (Table 1, Aguilera-Betti et al., 2020, Muñoz et al., 2020, Rozas et al., 2018). These sites were initially sampled according to dendroclimatological strategies, where dominant, separately standing trees were usually sampled; however, a sampling strategy similar to that used in the *N. macrocarpa* forests was applied in this study for the sampling of new *A. chilensis* trees. Most sampling sites are currently protected at different degrees, since they are included in priority areas for nature conservation. However, this protection status is relatively recent and most of the forests were outside the National Park Service before 1967, suffering some degree of human disturbance in the recent past, particularly by the impact of anthropogenic fires (González et al., 2018).

Wood samples were air-dried, glued onto wooden supports and polished with progressively finer sandpaper to visualize the anatomy of tree-ring boundaries. Tree rings were cross-dated through the synchrony of the narrow/wide ring pattern (Stokes and Smiley, 1996) by visual inspection under a stereomicroscope (×50 magnification). *N. macrocarpa* has semi-porous wood where the recognition of the ring boundary is facilitated by the presence of a thin layer of thick-walled fibers and marginal parenchyma in the latewood (Venegas-González et al., 2018b). *A. chilensis* wood is made of tracheids and the ring boundary is discernible by the radial flatten and greater thickness of the cell walls in the latewood (Roig, 1992; Rojas-Badilla et al., 2017). The ring widths were measured combining the two methodologies (i) a microscope mounted on a Velmex sliding stage incremental measuring machine (Bloomfield, NY, USA) and (ii) using an image software (Rasband, 1997), both at 0.01 mm resolution. We followed the Schulman (1956) shift convention for the Southern Hemisphere which assigns the annual calendar date of the ring to the year when the radial growth started. Although we are not aware of studies on cambial activity of these species, we believe that the growing season lasts from September to March, since the climatic conditions during this period have been identified as those with the highest incidence in the variability of the ring width for both species (Le Quesne et al., 2006; Venegas-González et al., 2018b).

The ring-width measurements were cross-correlated using visual and statistical techniques, such as the COFECHA program (Holmes et al., 1986; Grissino-Mayer, 2001), which compares the individual ring-width series with the master chronology resulted from the corrected series for each site. The cross-dating comparison is a necessary stage for the identification of missing and false rings, as well as other possible errors during the measurement process. All the tree-ring width measurements were standardized to remove non-climatic signals such as tree aging or growth deviations resulting from discrete growth incidents due to forest dynamics processes. We merged all the raw ring-width series for each species and ran ARSTAN v44h program (Cook, 1985) to produce the final chronologies. Through this program we standardized the individual series using either negative exponential, Hugershof or linear fitting detrending functions, depending on the best visual correspondence of fit (Cook et al., 1990). Detrended measurements were averaged using biweight robust mean (Cook et al., 1990). The "standard" chronologies were chosen, and no variance stabilization was used.

2.3. VS-Lite model of tree growth

2.3.1. Model description

VS-Lite is a simplified version of the Vaganov–Shashkin process-based model of tree growth (Fritts et al., 1991; Vaganov et al., 2006, 2011). For the full description of the model and the Bayesian algorithm of parameter estimation, we referred to the VS-Lite forward model version 2.3 (available at http://www.ncdc.noaa.gov/paleo/softlib/softlib.html, Tolwinski-Ward et al., 2013, 2011). The model simulates annual ring width according to the principle of the limiting factors, requiring latitude, monthly mean temperature, and monthly total precipitation as inputs. The representation of the individual cambial cells and the biological processes that govern them, both important components of the full VS model, are absent in VS-Lite. However, nonlinear climatic controls of tree radial growth are represented in VS-Lite in the form of threshold growth response functions and in implementation of the principle of limiting factors (Fritts, 1976), similarly to the VS model.

The VS-Lite model estimates monthly soil moisture from temperature and total precipitation data via the empirical one-layer Leaky Bucket model of hydrology (Huang et al., 1996). This hydrology scheme estimates evapotranspiration, surface runoff, and groundwater flow as empirical functions of the input data, subtracting them from incoming precipitation and adding the previous month's soil moisture to compute the present monthly soil moisture (Tolwinski-Ward et al., 2011). Snow dynamics are not considered in the model and thus all precipitation is assumed to be liquid. Seasonal insolation or day length is determined from site latitude and does not vary from year-to-year. For each year, the model simulates standardized (ageless) tree-ring width anomalies from the minimum of the monthly growth responses to temperature (gT) and moisture (gM), modulated by insolation (gE).

2.3.2. Model implementation

In this study, most of the tuneable model parameters (e.g., soil moisture, runoff, root depth) were set to the default values proposed in Tolwinski-Ward et al. (2011). The growth response functions for temperature (gT) and moisture (gM) in VS-Lite involved only two parameters: temperature (T1) or moisture (M1) threshold below which the growth will not occur, and the optimal temperature (T2) or moisture (M2) above which the growth is not limited by climate. Unlike the full version of the VS model, VS-Lite does not have an upper threshold in the growth response functions above which the influence of temperature and moisture turns negative. The growth function parameters were estimated for each site via Bayesian calibration evaluating the model 15,000 times for each site using three parallel Markov Chain Monte Carlo (MCMC) sequences with uniform prior distribution for each parameter and a white Gaussian noise model error (Tolwinski-Ward et al., 2013). The posterior median for each parameter was used to obtain the "calibrated" growth response for a given site. To compute annual ring widths, we integrated the overall simulated growth rates (i.e., the pointwise minimum of monthly gT, gM, and gE) over the period between previous-year March and current-year June. The CRU TS 4.00 gridded monthly mean temperature and precipitation data at 0.5°x0.5° spatial resolution (Harris et al., 2020) were used to calibrate the model. This included monthly values of precipitation and temperature for the period 1901–2016, derived by interpolation from quality-controlled station data. In the case of central Chile, most climate records start in the second half of the 20th century. However, the climate variability across central Chile is very coherent (e.g., Garreaud et al., 2017), hence, a handful of stations prior to 1960 gives a reasonable depiction of the climate state in the studied region. We spatially averaged the data for all grid points in the area between32.25–36.25°S and 70.25–71.25°W, that included all the study sites. We divided the analysis into two equal periods of 56 years (1901–1957, 1958–2014). We used the period 1901–1957 to calibrate the model and 1958–2014 to validate. Then we reverted the analysis, calibrating the model on 1958–2014 period and validating it on the 1901–1957 one. Finally, the model was calibrated

over the entire period 1901–2014, and then run using the calibrated parameters to produce a simulated tree-ring chronology that represented an estimate of the tree growth due to climatic variations.

2.4. Climate-growth relationships

Climate-growth relationships were assessed for the period 1901–2014 using two complementing methods: (i) correlation analysis (Fritts, 1976), and (ii) analysis of VS-Lite modeled patterns of partial growth rates due to soil moisture and temperature at monthly resolution. Since meteorological conditions of the previous year affect the growth of the following year when the growth ring is formed (Fritts, 1976), correlations were estimated with the climatic data from January of the year when tree ring formation started till April of the year when the tree ring formation ended. Previous studies showed that winter and spring months (May to October) represent key environmental conditions for the formation of wood in the studied species in MFCC (Le Quesne et al., 2006; Venegas-González et al., 2018b).

2.5. Climate forcing and tree growth projections

Tree growth projections were based on monthly values of temperature and precipitation from the output of 35 climate models, including those from the global CMIP-5 simulations (Taylor et al., 2012), the continental CORDEX simulations (Solman et al., 2013), and the regional model RegCM4 for Chile (Bozkurt et al., 2019). We downloaded all the future climate data from the web-site http://simulaciones.cr2.cl/. The spatial domain covers a rectangular area including the locations of all the tree-ring chronologies. All these simulations were initiated in the early or mid 20th century and extended at least until the year 2065. Until 2005 the models were integrated with the observed concentrations of GHG and atmospheric aerosols, so they followed the observed climate (mean values and variability). After 2006 the models were integrated by GHG concentrations that followed RCP2.6 and RCP8.5 emissions scenarios defined in the IPCC Fifth Assessment Report (Van Vuuren et al., 2011). RCP 8.5 represents a heavy GHG emissions scenario during the rest of the 21st century which implies that CO_2 concentration reaches 1, 100 ppm by 2100. On the contrary, RCP 2.6 is a lower-emissions scenario in which the increase in annual emissions is more gradual and declines after the mid-21st century (Pachauri et al., 2014).

Climate models give us an adequate representation of the mean climate and trend but their representation of the actual values in a given region can be biased by the imperfect representation of the earth system. These problems are present in the temperature field but even more marked in the case of precipitation over complex terrain, as the models – with their finite resolution – do not capture all the topographic features that can produce precipitation enhancement and rain shadows (Viale and Garreaud, 2015). To alleviate these problems, we followed a standard bias correction (see Bozkurt et al., 2019 for a review) using CRU TS 4.00 (Harris et al., 2020) as an observational dataset. For each calendar month (Jan, Feb, etc.) we calculated the long-term mean (1950–2005) of CRU TS temperature and precipitation across the spatial domain. Likewise, we calculated the monthly long-term mean of temperature and precipitation for each climate model for the common period 1950–2005. In the case of temperature, the bias correction factor is the difference in mean values. In the case of precipitation, the correction factor is the ratio between the observed and simulated mean values. We then applied these monthly mean correction factors to the actual (month/year) simulated values in both historical and future scenarios. We subsequently worked with these corrected climate simulations. The long-term mean of the corrected simulations in the historical period match with their observed counterparts.

As previously indicated, climate simulations project a warmer and drier future for central Chile (Bozkurt et al., 2019). Within the study area, by the year 2065 temperature rise will reach ~0.5 °C under RCP 2.6 and ~2.0 °C under RCP 8.5 (relative to the 1976–2005 baseline period, see also Fig. 2). The precipitation decreases from the baseline to the mid 21st century will range from ~5% under RCP 2.6 to ~20% under RCP 8.5 in the region. There is a consensus that, given an emission scenario, the mean temperature change will be more robust than the precipitation changes. In some regions of the world, different climate models even differ in the sign of the precipitation change. While uncertainty is indeed present in climate projections, central Chile stands out as a region where the drying trend is highly consistent among the models e.g., (Boisier et al., 2018, Seager et al., 2019). We also emphasize that using more than 30 climate models with different configuration results in a more robust estimate of likely changes in precipitation and temperature.

On the next step we forced the VS-Lite model with the projected future climate data. We used the output of each climate model (adjusted monthly temperature and precipitation) as an input to VS-Lite model. In this way, we acquired an ensemble of projected radial growths for each tree species. These ensembles were used to estimate the average and uncertainty. Prior to this, VS-Lite model was calibrated to the regional chronology of each species for the period 1901–2014. However, it should be noticed that when using parameter values derived from a calibration period for future growth projections, we utilize the underlying assumption of a limited ability of trees to adapt to climate changes.

We calculated the modeled growth for both the historical (1950–2005) and projected periods (2006–2065), according to the output data of the climate models. We divided the projected time period into four 15-year long periods: contemporary period (2006–2020), near (2021–2035), intermediate (2036–2050), and far future (2051–2065). To compare the effect of periods and scenarios on projected tree growth, we used linear mixed models (LMM). The data showed a normal distribution according to normal quantile-quantile (QQ plot) and residuals based on the values adjusted by the model (residual plot) (Fig. S1). We used scenario type (RCP 2.6 vs. RCP 8.5) and period (historical, contemporary, near, intermediate, and far future), and interactions among variables as fixed factors. We included the year as a random factor to take into account the temporal variability. We tested the differences using the post hoc least significant difference Fisher test. To perform this analysis, we used the LMM implementation of the *nlme* library in the R software (the *lme* function).

3. Results

3.1. VS-Lite model calibration and validation

The results of the robustness of the VS-Lite modeling are shown in Table 2, and the obtained model parameters in Table S3. Pearson correlation coefficients between modeled and measured annual tree growth were significant ($p < 0.05$) for all the experiments. Results did not change substantially when comparing calibration relative to validation period (Table 2). Interestingly, the modeled tree growth was almost identical for *N. macrocarpa* and *A. chilensis* ($r = 0.99$) tree-ring sources, while the correlation between the observed regional chronologies of these species was also high ($r = 0.59$) (Fig. 3). Together with the results of climatic response analyses from the following section, it emphasizes the similar climatic drivers of tree growth for both species.

3.2. Climate-growth relationships derived from VS-Lite modeling

Climatic responses of the regional chronologies of *N. macrocarpa* and *A. chilensis* showed similar features. Both species have the highest positive correlations with precipitation during the winter months prior to the growing season, and the highest negative correlations with temperature in November (Fig. 4 a,c; see also Fig. S3 for partial correlation analysis). Specifically, we found that the wettest months influenced radial growth in both species, especially from May to August in *A. chilensis* ($r \sim 0.40$, $p > 0.01$), and from May to July in *N. macrocarpa* ($r \sim 0.30$, $p > 0.05$), which was consistent with the marked seasonality

Fig. 2. Projected climate of central Chile (32–35°S – 70.5-71.5°). (a) Temperature and (b) Precipitation. Black – historical period, green – RCP 2.6, and red – RCP 8.5. Shading shows maximum and minimum values from all the scenarios; bold lines show average ensemble projections. (For interpretation of the references to colour in this figure legend, the reader is referred to the web version of this article.)

Table 2
Validation of the VL-Lite model. Coefficients of correlation between modeled and measured values are shown.

Species	1901–1957		1958–2014		1901–2014
	calibration	validation	calibration	validation	calibration
N. macrocarpa	0.52	0.52	0.63	0.57	0.59
A. chilensis	0.69	0.68	0.70	0.63	0.69

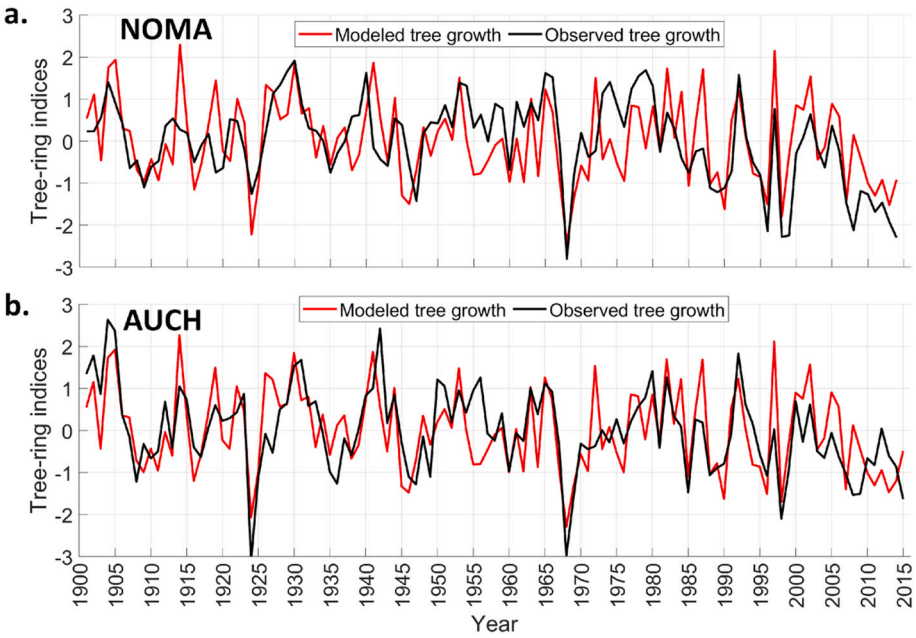

Fig. 3. Results of the VS-Lite model calibration and validation for (a) *N. macrocarpa* ($r = 0.59$), and (b) *A. chilensis* ($r = 0.69$), for the period 1901–2014.

of precipitation in this region (almost no rain occurs during austral summer months, December to February). In relation to the influence of mean air temperature, we observed a strong inverse correlation between radial growth and temperature at the beginning of the growing season in central Chile, as reflected in the beginning of the vascular cambium activity. Moreover, a stronger climate-growth association in *A. chilensis*, as compared to *N. macrocarpa*, was evidenced from higher correlation coefficients with climatic parameters (Fig. 4 a,c), and higher correlation

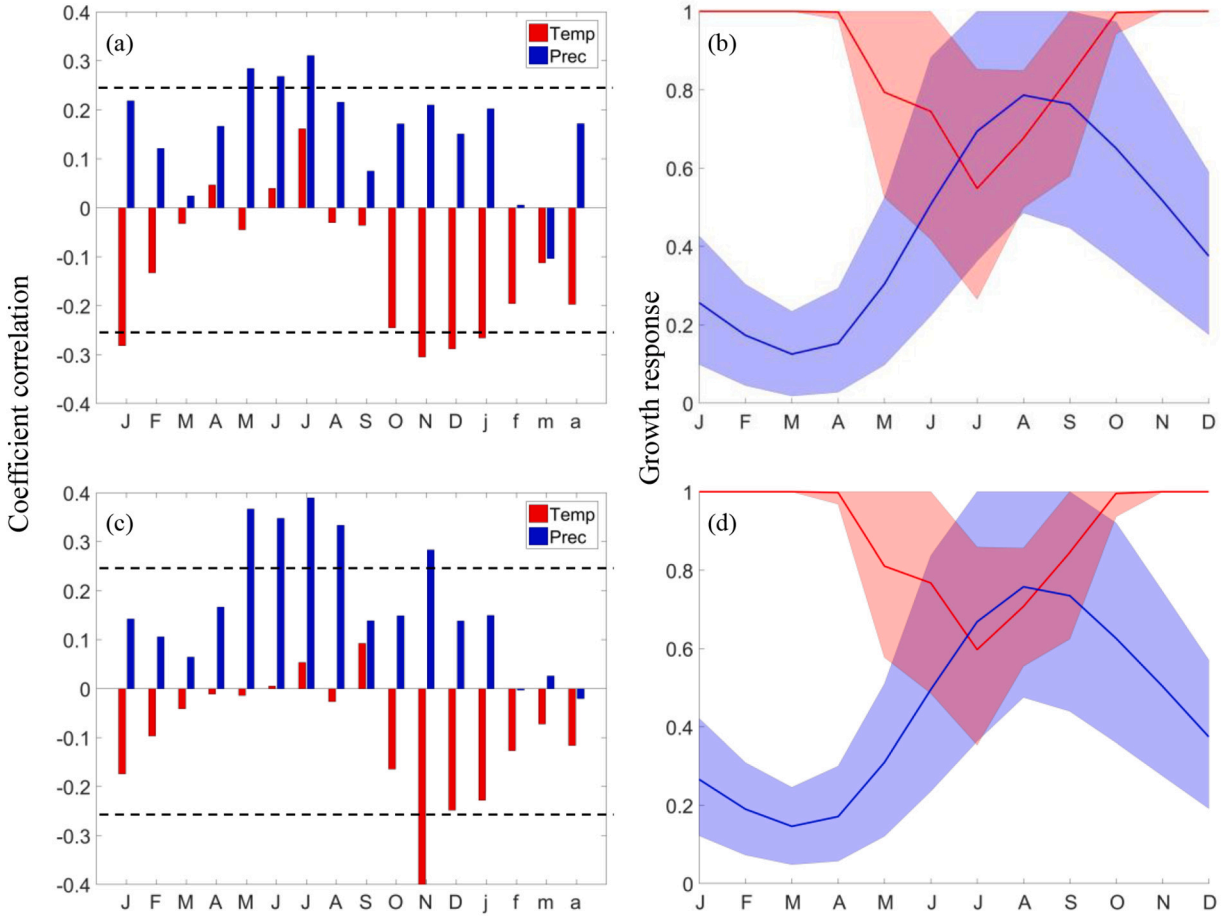

Fig. 4. Climate growth relationships from response function analysis (a,c) and VS-Lite modeling (b,d) for the period 1901–2014. Dashed horizontal lines indicate statistical significance at the 95% confidence level. In the panels (b,d) the monthly growth rates due to soil moisture (gM, blue) and temperature (gT, red) are shown (median, 2.5 and 97.5 percentiles). Results for *Nothofagus macrocarpa* are shown at the top (a,b), for *A. chilensis* at the bottom (c,d). Values of the gM and gT parameters close to 1 (y axis) indicate no growth limitation by climate. (For interpretation of the references to colour in this figure legend, the reader is referred to the web version of this article.)

coefficients between the observed and modeled tree growth (Fig. 3, Table 2).

Partial growth rates due to temperature and soil moisture acquired from VS-Lite modeling showed that for both species the main limiting factor for tree growth is soil moisture (Fig. 4 b,d) during most of the year. Only during July and August, the coldest months, low temperature becomes the main limiting factor for tree growth. Altogether, the results of climatic response analysis and VS-Lite modeling suggested that soil moisture driven by precipitation mainly during winter and spring and by evaporation during spring and summer is the primary limiting factor of radial growth of *A. chilensis* and *N. macrocarpa* in the region.

3.3. Projections of future tree growth

We compared the observed (1901–2014) and simulated (1950–2065) tree growth of *N. macrocarpa* and *A. chilensis* (Fig. 5). The historical and future radial growth simulations were very similar for both tree species, which is not surprising considering that they come from the same climatic region (Fig. 1), and they have similar growth response to climate variability (Fig. 4). This aspect was also sustained by the fact that the VS-Lite model only accounts for the climate-driven component of tree growth. On this basis, we combined the projections of tree growth for both tree species. We found substantial changes in ensemble mean tree growth under the RCP8.5 and RCP2.6 scenarios, which appeared to be significantly different compared to the growth of the historical period (Fig. 5).

The LMM results showed that the periods, scenarios and interaction between them had the strongest effect on modeled tree growth, with 80% of explained variance (50% due to the fixed effects) (Table 4). We observed that starting from the intermediate period (2035–2054) there was a significant difference between the RCP 2.6 and RCP 8.5 scenarios, with lower estimated tree growth for the latter one. For the RCP 2.6 scenario, we observed that at the beginning of the intermediate period (2036–2050) the estimated tree growth was significantly lower relative to the contemporary and historical period (Fig. 6). Under a more extreme RCP 8.5 scenario the situation is even more dramatic because the estimated tree growth has a greater intensity of decrease. Statistically significant differences with contemporary and historical periods are pronounced starting from the near future period (2021–2035, Fig. 6). For example, the mean projected tree growth for the far future corresponds to the 21th percentile of the modeled tree growth for the instrumental period (1901–2015), which means that it was lower than 79% of all the values for this period (Table 3).

4. Discussion

Our results demonstrate that projected climate change according to the RCP 2.6 and RCP 8.5 scenarios will have a negative impact on forest growth in the MFCC, causing a regional-scale forest decline. Previous studies showed the sensitivity of tree growth to climate variability in central Chile, using ecological assessments (e.g. Gutierrez et al., 2008) and climate reconstructions (e.g. Le Quesne et al., 2009, 2006) derived

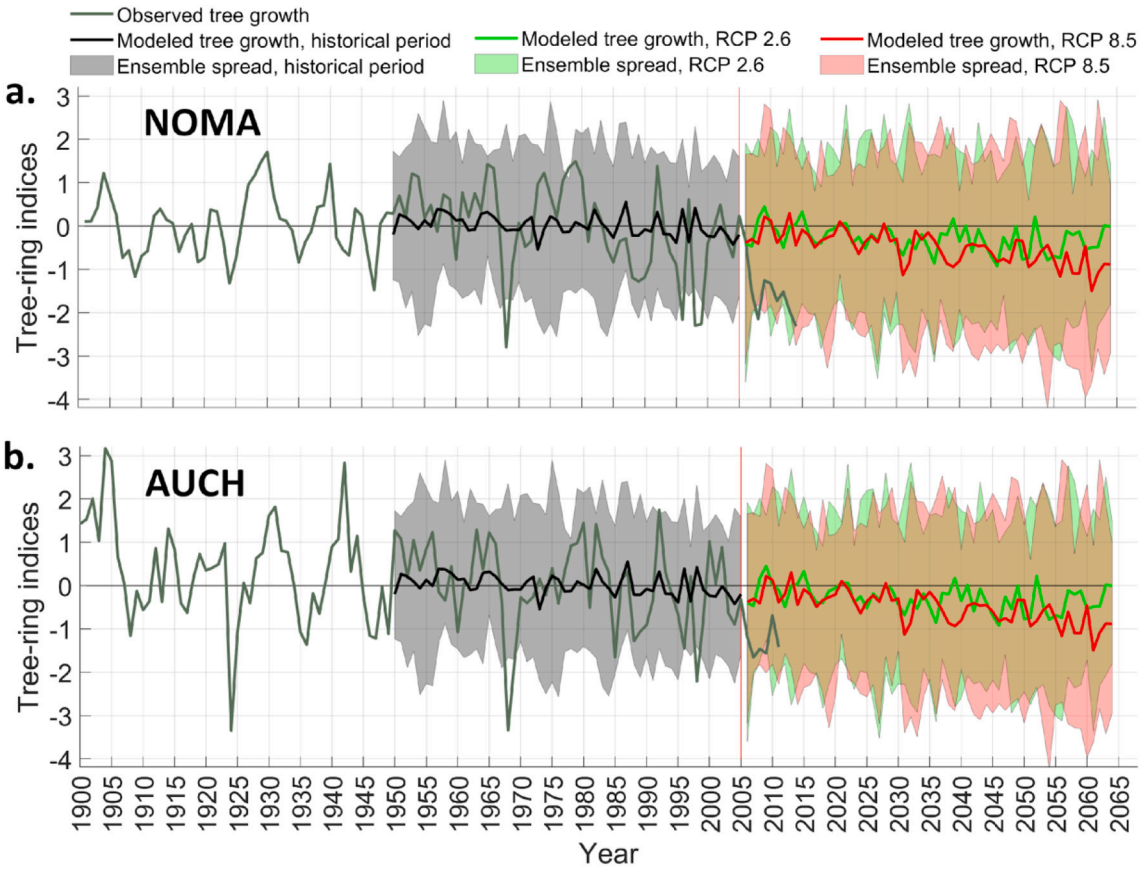

Fig. 5. Observed and modeled tree-ring indices for the two studied species according to the two IPCC scenarios. (a) *Nothofagus macrocarpa*, (b) *Austrocedrus chilensis*. Modeled growth in the historical period is not supposed to reproduce year-to-year dynamics of the observed growth, just like modeled climatic parameters do not capture observed year-to-year changes. At the same time, most of the observed growth values are inside the ensemble envelope. Note that *N. macrocarpa* and *A. chilensis* are indistinguishable in terms of modeled growth.

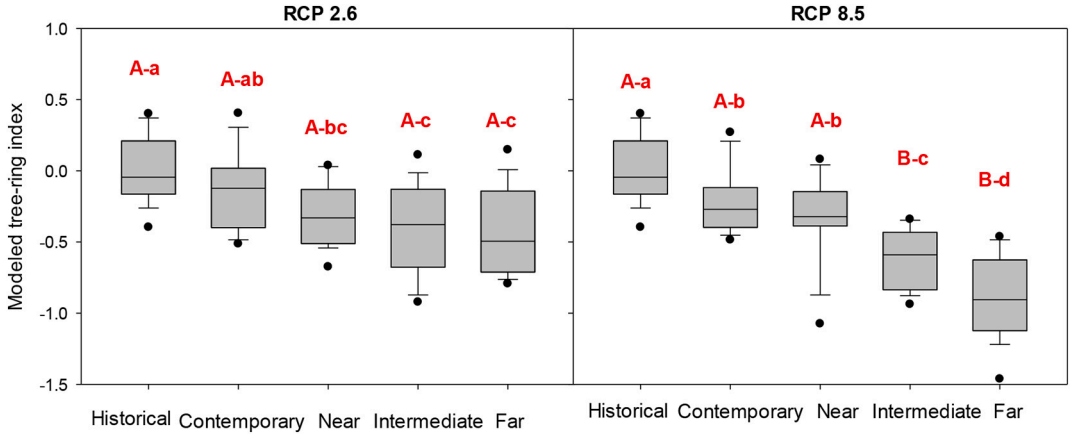

Fig. 6. Difference among projected tree growths for 15-year periods under the two climate scenarios: RCP 2.6 (left panel) and RCP 8.5 (right panel), using observational and modeled climate data. Contemporary: 2006–2020, Near future 2021–2035, Intermediate future: 2036–2050, and Far future: 2051–2065. Different letters indicate significant differences among the tree ring indices according to Fisher test (both scenarios with $p < 0.001$). Capital letters mark differences between the two scenarios in the same period; lowercase letters mark differences between periods in the same scenario.

from tree rings. But to the best of our knowledge, however, none had ventured to assess tree growth projections for the future in a climate change context. High radial growth sensitivity of the studied tree species to climate variability in MFCC provided a reliable basis for identifying the vulnerability level of these ecosystems to future climate change. Furthermore, the novelty of this research is that the chronologies of the entire natural distribution of *N. macrocarpa* have been considered, which is the northernmost distributed *Nothofagus* species. Our study also included the northernmost *A. chilensis* populations, both in the Coastal and Andes Mountains (Armesto et al., 2007), representing its trailing edge due to increased drought conditions. Thus, we argue that our results provide relevant information about vulnerability of mountain forests of unique Mediterranean-type ecosystems of South America to climate change.

Table 3
Descriptive statistics of projected tree-ring index of regional chronology to Contemporary: 2006–2020, Near future 2021–2035, Intermediate future: 2036–2050, and Far future: 2051–2065 periods, according to scenarios RCP 2.6 and RCP 8.5.

Scenarios	Mean (SD)	Min	Max	Median	Q1	Q3	PRC*
RCP 2.6							
Contemporary	−0.12 (0.28)	−0.53	0.42	−0.15	−0.42	0.01	48
Near future	−0.31 (0.23)	−0.74	0.03	−0.28	−0.47	−0.09	44
Intermediate future	−0.39 (0.32)	−0.95	0.14	−0.39	−0.64	−0.12	41
Far future	−0.43 (0.32)	−0.81	0.17	−0.51	−0.76	−0.15	40
RCP 8.5							
Contemporary	−0.21 (0.32)	−1.13	0.07	−0.34	−0.41	−0.12	46
Near future	−0.35 (0.28)	−0.53	0.42	−0.15	−0.42	0.01	42
Intermediate future	−0.61 (0.24)	−0.97	−0.18	−0.59	−0.86	−0.43	30
Far future	−0.88 (0.32)	−1.53	−0.39	−0.91	−1.12	−0.61	21

* the mean value of tree growth projection for the period corresponds to this percentile of the distribution of modeled values for the instrumental period (1901–2014).

Table 4
Results of linear mixed model of tree-growth projections to regional chronology (*A. chilensis* and *N. macrocarpa*), under the scenario (RCP 2.6 vs. RCP 8.5), period (Contemporary, Near future, Intermediate future, and Far future), and their interaction as fixed factors and year as random factors. Data represent the degrees of freedom (df num, df den), the *F*-statistic with the associated *P*-value of significance (significant effects, $P < 0.05$).

Fixed effects	Df num	Def den	*F*	*P*
Intercept	1	114	163.35	<0.0001
Scenario	4	107	33.94	<0.0001
Period	1	107	31.98	<0.0001
Scenario x Period	4	107	9.24	<0.0001
R^2*	0.80 (0.50)			

* The marginal and conditional R^2 values for each model are also shown (values in parentheses indicate the marginal R^2 due to the fixed factors).

4.1. Climatic response of tree-ring chronologies in MFCC

Although the studied tree-ring chronologies are located at different sites, they share a common regional response pattern to climate variability. Conditions of higher rainfall during the austral winter (mainly between June and August) combined with mild spring and summer temperatures stimulate the vegetative activity in both species (Fig. 4a). This indicates that winter precipitation causes favorable conditions for moisture recharge in soils before and after the cambial activity starts (ca. October), while warm spring- early summer temperatures constrain tree growth (Fig. 4b), most probably by the increase in evapotranspiration. This is due to the Mediterranean-type precipitation seasonality in the region, with most of the moisture supply during the winter months and an almost completely absent precipitation during the warm summer months. Here it is important to mention that partial growth rates due to soil moisture modeled in VS-Lite also included the inverse temperature signal, as the model calculates moisture loss due to evaporation on the base of temperature.

4.2. Recent and future climate variability in Central Chile and its consequences for the forests of MFCC

The most pronounced temperature increase in Chile has been identified at high elevations (Vuille et al., 2015), resulting in a rise of the zero-degree isotherm that affected the snow contribution, critical for aquifer and soil recharge (Carrasco et al., 2008). Additionally, these phenomena have hastened the decrease of snowpack and glaciers in the Andes and Coastal mountains for both their size and volume (Dussaillant et al., 2019), with consequent runoff decreases in mountain rivers, making ecosystems and societies that depend on them more vulnerable (Ragettli et al., 2016). The temperature-driven phenomena act in concert with a marked decline in rainfall at lowlands and snowfall over the Andes. Changes in snow contribution to water soil recharge could further aggravate the complex scenario for these species in the near future, particularly for tree populations located in the Coastal mountain tops (*Nothofagus macrocarpa*), considering the importance of soil moisture for radial growth of these trees (Venegas-González et al., 2018a). Boisier et al. (2016) and Garreaud et al., 2020 estimated that as much as a quarter of the rainfall deficit during the last decade is attributable to anthropogenic climate change, mediated by altered mid- to high-latitude circulation in the Southern Hemisphere. This resulted in a multi-year drought of unprecedented length in recent history on both sides of the central Andes (Garreaud et al., 2017; Rivera et al., 2017). A drought of such intensity has affected not only the regional hydroclimate, but also the vegetation (Garreaud et al., 2017; Miranda et al., 2020), forest growth at different ages (Venegas-González et al., 2019), and crops (Zambrano et al., 2016).

Climate change projections indicate a year-round drying and warming of central-south Chile. This situation may reach up to 30% rainfall reduction and 3.5 °C temperature rise by the end of the 21st century under a heavy emission scenario (RCP 8.5; Bozkurt et al., 2018). In this context, protracted droughts like the one occurring since 2010 are likely to become more frequent in the near future (Boisier et al., 2016). Extreme climate events have been documented as the major drivers of forest decline and mortality, but they are also responsible for other crucial ecological processes in the studied species. For example, droughts have affected the seed patterns of *Nothofagus obliqua*, a dominant deciduous tree species in lowland MFCC, increased tree mortality and decreased recruitment (unpublished results). Recent dry and hot episodes have been linked to forest decline in *Nothofagus* spp. and *A. chilensis* forests in central Chile and northern Patagonia (Amoroso et al., 2015; Fajardo et al., 2019; Rodríguez-Catón et al., 2019; Venegas-González et al., 2018b). Episodes of extreme weather can have harmful consequences on the forest ecosystems of the region, such as the increase in populations of defoliating insects or extensive and repeated fires in central-south Chile. In this sense, the increase in defoliation events by *Ormiscodes* moth on *Nothofagus pumilio* north Patagonian forests were linked to regional warming (Estay et al., 2019; Paritsis and Veblen, 2011). This alerts to the possible increased vulnerability of the *N. macrocarpa* forests in the future, since it is known that this defoliator is also associated with *N. macrocarpa* in central Chile (Altmann and Claros, 2015). It is also known that low-intensity fire events have been a recurring phenomenon affecting both *A. chilensis* and *N. macrocarpa* forests during the past 1000 years, indicating that these forests are resilient to such a disturbance (Rozas et al., 2018). However, the simultaneous interaction of higher temperatures and lower precipitation during several consecutive years have increased the probability of forest fires in the region (González et al., 2018; Urrutia-Jalabert et al., 2018), consequently increasing the vulnerability of *A. chilensis* and *N. macrocarpa* forests.

Our results indicate that even considering the most benign scenario (RCP 2.6), there will be a significant decrease in the projected radial tree

growth compared to the current period (Fig. 5). For the high emissions scenario (RCP 8.5) the situation is projected to be even worse, since it is expected that by the year 2065 the median tree growth will correspond to the lower quartile of the values observed for the last century. Similarly, to other Mediterranean forests (Dorado-Liñán et al., 2019; Sánchez-Salguero et al., 2017a), our results suggest that MFCC populations of *A. chilensis* and *N. macrocarpa*, currently subjected to warm and dry conditions, will be seriously vulnerable toward the end of the 21st century, especially due to the dramatic forecasted temperature increase during the growth season.

4.3. Possible changes in water use efficiency and tree growth projections

Several forest ecosystems have increased the internal water use efficiency (iWUE) during the last decades, as evidenced by the carbon isotope ($\delta^{13}C$) contents in tree rings (e.g. Guerrieri et al., 2019; Keenan et al., 2013). This indicates an optimal balancing of trees between carbon gains and water costs. The increase in iWUE has favored the tree growth in some tree species (e.g. Battipaglia et al., 2013), but in other circumstances positive trends in iWUE do not translate into enhanced tree growth (e.g. Lévesque et al., 2014). The relationship between iWUE and radial growth in Mediterranean species from central Chile has not been studied yet. However, it was shown by Tognetti et al. (2014) that for other *Nothofagus* species of Chile, iWUE and basal area are both increasing throughout the 20th century. Hence, we believe that part of the regional decline of mountain forests that we projected could be compensated by CO_2 fertilization through the increased iWUE. Moreover, in the Mediterranean forests of northern Argentinean Patagonia, Arco Molina et al. (2019) found that in the conifer species *Araucaria araucana* both the iWUE and intercellular CO_2 concentrations (C_i) registered an increase of 33% and 32%, respectively, during the last century. These changes in iWUE were strongly related with changes in atmospheric CO_2 and significantly affected by mean summer maximum temperature increase, both in short and long-term timescales. Even though studies on carbon isotope composition ($\delta^{13}C$) in tree rings of *A. chilensis* are currently being developed, the preliminary results show an increase in iWUE and Ci to site ELA (personal communication).

4.4. Expected shift in vegetation of relict forests of Central Chile

It is well known that for every 100 m of increase in altitude there is a general decrease in temperature of 0.5–0.6 °C (Körner and Paulsen, 2004). Hence, it is expected that continuity in the global increase of temperature will push up the limiting environmental conditions of vegetative growth. It has been estimated that an increase in temperature of 1 °C will cause conditions for Mediterranean vegetation to rise about 170 m from its current altitude, that equates to a poleward displacement of more than 140 km (Jump et al., 2009). Evidence of forests alteration forced by temperature increase is already being observed, or at least expected, in various parts of the world; for example, temperate forests in Spain are being progressively replaced by Mediterranean tree species (Penuelas et al., 2007). In California, with temperature increases above 2 °C, the replacement of scrublands for desert grasslands and evergreen conifers for mixed evergreen forests is projected (Hayhoe et al., 2004). Inclusive enhanced fitness and greater herbivore resistance of non-native plants in mountain ecosystems are expected (Alexander et al., 2016). According to Bambach et al. (2013), the environmental variables that best explain the species distribution in MFCC are precipitation and temperature of the warmest months. Some evidence indicates that certain *Nothofagus* forests could adapt to higher elevations as conditioned to a new climatic situation. Mathiasen and Premoli (2016) have suggested the evolutionary potential of low-elevation genotypes of *N. pumilio* to colonize higher-altitude sites. Even though this could not apply to the coastal range of *N. macrocarpa* forests, as they currently occupy the highest sites and could not rise further, this could happen with the Andean populations (Mathiasen et al., 2020). Therefore, *Austrocedrus chilensis* forests positioned at middle altitudes of the mountain range are probably in more favorable conditions. In case of forest upslope migrations induced by global warming, high-elevation populations may be potentially outperformed by the low-elevation ones during this process, leading to a gradual replacement of these genotypes (Mathiasen and Premoli, 2016). This could be the case of *Austrocedrus*, a species that although it uses very particular soils to establish, its growth rates are comparatively lower than those of other tree species in the Mediterranean forests. Thus, species' interactions (e.g. competition, facilitation) will play a fundamental role for either the coexistence or replacement of species under projected climatic changes in this region.

4.5. Limitations of the approach used and perspectives

Our methodology, where a set of parameter values derived from a calibration period is used for future growth projections, utilizes an assumption of a limited ability of trees to adapt to climatic changes. This assumption may be incorrect, resulting in changing parameters of VS-Lite model in the future at certain sites and for certain species. Nevertheless, our results of model-to-data comparison for different calibration periods demonstrated robustness of the model and testified the methodology used, at least for the climatic changes that are comparable to those that happened throughout the 20th century.

In this study we focused on tree growth projections at regional scale. In preliminary experiments with VS-Lite (not shown here) we also applied the model on a site-by-site level, but in this case the model decreased its performance. This is in accordance with other known cases of application of the VS-Lite model worldwide (Breitenmoser et al., 2014), where the modeling results were better when grouping the chronologies in regions of 200–600 km wide compared to the results for separate chronologies. This may be connected to the coarse spatial resolution of gridded CRU TS climate dataset that fails to capture fine-scale details of the temperature and precipitation fields (Breitenmoser et al., 2014), as well as to the lack of model's parameters tuning. For example, soil moisture calculations based on simple bucket size are very sensitive to parameter selection. Therefore, the good model performance that we achieved at regional scale points to the possibility of application of general model setting for regional studies. However, future studies based on site-by-site parameter tuning can give more insights concerning biogeographical variability in tree growth.

Another caveat is that Thornthwaite approach of estimating evapotranspiration from surface temperature starts to break down under future temperature changes outside the normalization interval (Smerdon et al., 2015). Huang's Leaky Bucket model implemented in VS-Lite uses the Thornthwaite approximation, and therefore it is likely that future drying within VS-Lite itself is overestimated. In future studies it is preferable to use soil moisture directly from the climate models in order to reduce possible biases connected to this approximation. In the case of Central Chile, it would be also desirable to calculate soil moisture based on in situ measurements to validate if certain climate models give appropriate results.

To better understand how seasonality of projected climatic changes affects projected tree growth, we performed sensitivity tests with constant temperature and precipitation, except for one parameter (temperature or precipitation) and one season (DJF, MAM, JJA or SON). The results are presented in Fig. S2. Tree growth projections based on varying climatic parameters for different seasons confirm agreement of VS-Lite modeling results with growth-to-climate response analysis (Fig. 4a,c). Specifically, an increase in DJF temperatures leads to decrease in tree growth, which is in accordance with negative correlations of tree growth with temperature in October-to-February period (Fig. 4a,c). Meanwhile, winter temperature, which is the main limiting factor in winter months according to VS-Lite modeling results (Fig. 4b, d), increases in the projections, and hence stops to limit tree growth in these months. The overall increase of projected tree growth that is seen

for the experiment with constant precipitation and varying temperature (Fig. S2) is driven by autumn and winter temperature increase, as the relative cumulative growth increase due to autumn and winter temperature increase is larger than the growth decrease due to summer temperature increase. At the same time, changing spring temperatures by their own do not significantly alter tree growth (Fig. S2).

The results for varying precipitation show that the projected decrease in tree growth is mostly due to decrease in projected JJA precipitation, which is in accordance with positive correlations of tree growth with MJJA precipitation (Fig. 4a,c). At the same time, variations in projected summer precipitation have almost no effect on projected tree growth (Fig. S2).

On one hand, the results of sensitivity tests are consistent with growth-to-climate response analysis. But on the other hand, they detect another limitation of our approach – the probable necessity to change in time the growing season window, which is another parameter of VS-Lite model. In this study we used the whole year from April to April to integrate tree growth. This approach showed robustness in the calibration and validation tests for the 20th century. However, a more rigorous approach with varying growth season length must be considered in future studies to account for amplified projected climatic changes. It probably must exclude from the integration the winter period when the trees are dormant, as well as to account somehow for probable changes in growing season length with changing climate. Concerning this study, the discussed changes in methodology would futher reduce the projected tree growth because of the exclusion of some months with increased growth from the integration period.

Another critical climatic factor that would be good to consider in future studies is winter snow accumulation. It is indeed important for better water balance estimates (although snow accumulation is not included into the VS-Lite model hydrology block). Winter snow accumulation is also crucial in the growth dynamics of both species, as seed germination and successful recruitment depend on snow cover (Cruz, 2015; Gajardo, 2001). The expected decreased snowpack accumulation and earlier spring melting during the next decades could induce earlier xylogenesis resumption, and thereby force changes in the start and duration of the vegetative period (González-Reyes et al., 2017; Masiokas et al., 2006), exposing plants to risks of late frosts and long periods of water deficit (Arco Molina et al., 2019; Hadad et al., 2019).

The VS-lite model used here does not account neither for regeneration dynamics, nor for precipitation accumulation as snow, nor for the possible increased CO_2 effect on radial tree growth. Nevertheless, the fact that VS-Lite model was capable of reproducing the observed data on tree growth decline for the period between 2010 and 2018, which was forced by long-term precipitation decrease (Fig. 3), is another important justification of the model's performance that supports the use of VS-Lite for tree growth projections in the region.

One of the possible ways to overcome some of these problems is the use of more elaborated process-based models (see Guiot et al., 2014 for a list of candidates). However, such an improvement will comprise increased data and computational requirements, and might even question the robustness of the generated projections. For example, Gea-Izquierdo et al. (2017) used the MAIDEN model which accounts for water and carbon cycles, as well as tree compartments, and uses daily climate data as inputs. However, in that study it was impossible to perform model cross-validation on independent periods because of the lack of the data. Hence, comparative simplicity of the VS-Lite model can also be an important advantage, especially in case of limited availability of data for calibration and verification.

Another important factor that VS-Lite does not capture is tree mortality. The model continues to create dimensionless tree-ring indices as long as temperature and calculated soil moisture exceed corresponding parameters T1 and M1. However, even interrupted, modeled tree growth continues on the consecutive years provided that temperature and soil moisture increase. Since VS-Lite captures neither carbon starvation nor hydrologic failure, it is possible that changing climate conditions could lead to tree mortality at one moment in the projection period.

It should be also taken into account that the VS-Lite model does not include growth decline due to massive outbreaks caused by insects or pathogens, even though this incidence has been frequently associated with an intensification of heat. Future scenarios of climate change may trigger or accentuate physiological reactions that accelerate or intensify the observed decreases in growth. Consequently, future studies should include, beside demographic processes driving natural dynamics, such as mortality and regeneration, the use of stable isotopes and wood anatomy to evaluate possible physiological changes, paying attention to identification of functional adaptations of MFCC to climate change.

5. Conclusions

Our results showed that mountain relict forests of MFCC are vulnerable to future climate change, both under the moderate (RCP 2.6) and the high (RCP 8.5) GHG emission scenarios, as evidenced by regional-wide decline projections of growth in *N. macrocarpa* and *A. chilensis* trees. If the high emission scenario will be attested (RCP 8.5), tree growth is likely to be dramatically reduced by the second half of the 21st century (2051–2065), reaching at the 21th percentile of the tree growth reproduced by the VS-Lite model for the instrumental period (1901–2015). The projected decline in tree growth indicates serious risks in dynamics and survival of these forests in relatively short periods of time, so alerts are given about this situation which may require urgent counteracting strategies to minimize the deleterious effects of global change on vegetation in this region. The present study gives us a starting benchmark to analyze other factors that may affect forest vulnerability in MFCC in the context of climate change. Future research is needed to recognize sites and individual trees with greater possibilities of adaptation to drought conditions in mountain MFCC forests. This could be an important input in restoration and conservation projects to mitigate the effects of climate change.

Declaration of Competing Interest

None.

Acknowledgements

We sincerely thank five anonymous reviewers for valuable comments and suggestions to earlier versions of the manuscript. VM acknowledges IANIGLA-CONICET from Argentina for the postdoctoral fellowship that made this study possible. The assessment of the projections and the development of the methodology were supported by the Russian President Grant MK-3844.2019.5 and by the Russian State Assignment Project 0148-2019-0004. AVG thanks FONDECYT 11180992 and The Rufford Small Grants for Nature Conservation (25822-2). AGG was supported by Programa Bosques Andinos and FONDECYT 1200468. AAM was supported by FONDECYT 1201714 and FONDAP 15110009. CLQ was supported by FONDECYT 1181956.

Appendix A. Supplementary data

Supplementary data to this article can be found online at https://doi.org/10.1016/j.gloplacha.2020.103406.

References

Aguilera-Betti, I., Lucas, C., Ferrero, M.E., Muñoz, A.A., 2020. A network for advancing dendrochronology, dendrochemistry and dendrohydrology in South America. Tree-Ring Res. 76 (2), 94–101.

Alexander, J.M., Lembrechts, J.J., Cavieres, L.A., Daehler, C., Haider, S., Kueffer, C., Liu, G., McDougall, K., Milbau, A., Pauchard, A., 2016. Plant invasions into mountains and alpine ecosystems: current status and future challenges. Alp. Bot. 126, 89–103.

Allen, C.D., Macalady, A.K., Chenchouni, H., Bachelet, D., McDowell, N., Vennetier, M., Kitzberger, T., Rigling, A., Breshears, D.D., Hogg, E.H.T., 2010. A global overview of drought and heat-induced tree mortality reveals emerging climate change risks for forests. For. Ecol. Manag. 259, 660–684.
Allen, C.D., Breshears, D.D., McDowell, N.G., 2015. On underestimation of global vulnerability to tree mortality and forest die-off from hotter drought in the Anthropocene. Ecosphere 6, 1–55.
Altmann, S.H., Claros, S., 2015. Insect abundance and damage on the deciduous *Nothofagus macrocarpa* increase with altitude at a site in the Mediterranean climate zone of Chile. Austral Entomol. 54, 402–410.
Amoroso, M.M., Daniels, L.D., Villalba, R., Cherubini, P., 2015. Does drought incite tree decline and death in *Austrocedrus chilensis* forests? J. Veg. Sci. 26, 1171–1183.
Anderegg, W.R.L., Schwalm, C., Biondi, F., Camarero, J.J., Koch, G., Litvak, M., Ogle, K., Shaw, J.D., Shevliakova, E., Williams, A.P., 2015. Pervasive drought legacies in forest ecosystems and their implications for carbon cycle models. Science 349, 528–532.
Arco Molina, J.G., Helle, G., Hadad, M.A., Roig, F.A., 2019. Variations in the intrinsic water-use efficiency of north Patagonian forests under a present climate change scenario: tree age, site conditions and long-term environmental effects. Tree Physiol. 39, 661–678.
Armesto, J., Arroyo, M.T.K., Hinojosa, F., 2007. The Mediterranean Environment of Central Chile, The physical Geography of South America. Oxford University Press on Demand, pp. 184–199.
Arroyo, M.T.K., Armesto, J.J., Squeo, F., Gutiérrez, J., 1993. Global Change: The Flora and Vegetation of Chile. Earth Syst. Response to Glob. Chang: Contrasts Between North South Am, pp. 239–263.
Baldwin, H., 2018. Nothofagus macrocarpa. In: The IUCN Red List of Threatened Species 2018 e.T96478456A96480000.
Bambach, N., Meza, F.J., Gilabert, H., Miranda, M., 2013. Impacts of climate change on the distribution of species and communities in the Chilean Mediterranean ecosystem. Reg. Environ. Chang. 13, 1245–1257.
Barria, P., Rojas, M., Moraga, P., Muñoz, A., Bozkurt, D., Alvarez-Garreton, C., 2019. Anthropocene and streamflow: long-term perspective of streamflow variability and water rights. Elem. Sci. Anth. 7, 2.
Battipaglia, G., Saurer, M., Cherubini, P., Calfapietra, C., McCarthy, H.R., Norby, R.J., Francesca Cotrufo, M., 2013. Elevated CO_2 increases tree-level intrinsic water use efficiency: insights from carbon and oxygen isotope analyses in tree rings across three forest FACE sites. New Phytol. 197, 544–554.
Björklund, J., Rydval, M., Schurman, J.S., Seftigen, K., Trotsiuk, V., Janda, P., Mikoláš, M., Dušátko, M., Čada, V., Bače, R., 2019. Disentangling the multi-faceted growth patterns of primary *Picea abies* forests in the Carpathian arc. Agric. For. Meteorol. 271, 214–224.
Boisier, J.P., Rondanelli, R., Garreaud, R.D., Muñoz, F., 2016. Anthropogenic and natural contributions to the Southeast Pacific precipitation decline and recent megadrought in central Chile. Geophys. Res. Lett. 43, 413–421.
Boisier, J.P., Alvarez-Garretón, C., Cordero, R.R., Damiani, A., Gallardo, L., Garreaud, R. D., Lambert, F., Ramallo, C., Rojas, M., Rondanelli, R., 2018. Anthropogenic drying in central-southern Chile evidenced by long-term observations and climate model simulations. Elem. Sci. Anth. 6, 74.
Boninsegna, J.A., Argollo, J., Aravena, J.C., Barichivich, J., Christie, D., Ferrero, M.E., Lara, A., Le Quesne, C., Luckman, B.H., Masiokas, M., Morales, M., Oliveira, J.M., Roig, F., Srur, A., Villalba, R., 2009. Dendroclimatological reconstructions in South America: a review. Palaeogeogr. Palaeoclimatol. Palaeoecol. 281, 210–228.
Bowman, D.M.J.S., Moreira-Muñoz, A., Kolden, C.A., Chávez, R.O., Muñoz, A.A., Salinas, F., González-Reyes, Á., Rocco, R., de la Barrera, F., Williamson, G.J., 2019. Human–environmental drivers and impacts of the globally extreme 2017 Chilean fires. Ambio 48, 350–362.
Bozkurt, D., Rojas, M., Boisier, J.P., Valdivieso, J., 2018. Projected hydroclimate changes over Andean basins in central Chile from downscaled CMIP5 models under the low and high emission scenarios. Clim. Chang. 150, 131–147.
Bozkurt, D., Rojas, M., Boisier, J.P., Rondanelli, R., Garreaud, R., Gallardo, L., 2019. Dynamical downscaling over the complex terrain of southwest South America: present climate conditions and added value analysis. Clim. Dyn. 53, 6745–6767.
Breitenmoser, P.D., Brönnimann, S., Frank, D., 2014. Forward modelling of tree-ring width and comparison with a global network of tree-ring chronologies. Clim. Past 10, 437–449.
Burger, F., Brock, B., Montecinos, A., 2018. Seasonal and elevational contrasts in temperature trends in Central Chile between 1979 and 2015. Glob. Planet. Chang. 162, 136–147.
Carrasco, J.F., Osorio, R., Casassa, G., 2008. Secular trend of the equilibrium-line altitude on the western side of the southern Andes, derived from radiosonde and surface observations. J. Glaciol. 54, 538–550.
Castor, C., Cuevas, J.G., Arroyo, M.T.K., Rafii, Z., Dodd, R., Peñaloza, A., 1996. *Austrocedrus chilensis* (D. Don) Pic.-Ser et Bizz. (Cupressaceae) from Chile and Argentina: monoecious or dioecious. Rev. Chil. Hist. Nat. 69, 89–95.
Charney, N.D., Babst, F., Poulter, B., Record, S., Trouet, V.M., Frank, D., Evans, M.E., 2016. Observed forest sensitivity to climate implies large changes in 21st century North American forest growth. Ecology Letters 19, 1119–1128.
Chen, P.Y., Welsh, C., Hamann, A., 2010. Geographic variation in growth response of Douglas-fir to interannual climate variability and projected climate change. Glob. Chang. Biol. 16, 3374–3385.
Cook, E., 1985. A Time Series Analysis Approach to Tree Ring Standardization. Lamont-Doherty Geol. Obs. University of Arizona, Tucson (AZ), p. 171.
Cook, E.R., Briffa, K., Shiyatov, S., Mazepa, V., 1990. Tree-ring standardization and growth-trend estimation. Methods dendrochronology. Appl. Environ. Sci. 104–123.
Cruz, G., 2015. Comunidades de ciprés de la cordillera en el Alto Cachapoal. In: Cruz, G. (Ed.), Ciprés de La Cordillera (*Austrocedrus chilensis* (D. Don) Pic. Serm. et Bizarri): Antecedentes Ecológicos Para La Conservación de Las Comunidades En El Alto Cachapoal. Universidad de Chile, Facultad de Ciencias Forestales y de la Conservación …, Santiago, pp. 54–128.
Donoso, C., 1982. Reseña ecológica de los bosques mediterráneos de Chile. Bosque 4, 117–146.
Dorado-Liñán, I., Piovesan, G., Martínez-Sancho, E., Gea-Izquierdo, G., Zang, C., Cañellas, I., Castagneri, D., Di Filippo, A., Gutiérrez, E., Ewald, J., 2019. Geographical adaptation prevails over species-specific determinism in trees' vulnerability to climate change at Mediterranean rear-edge forests. Glob. Chang. Biol. 25, 1296–1314.
Dussaillant, I., Berthier, E., Brun, F., Masiokas, M., Hugonnet, R., Favier, V., Rabatel, A., Pitte, P., Ruiz, L., 2019. Two decades of glacier mass loss along the Andes. Nat. Geosci. 12, 802–808.
Estay, S.A., Chávez, R.O., Rocco, R., Gutiérrez, A.G., 2019. Quantifying massive outbreaks of the defoliator moth *Ormiscodes amphimone* in deciduous Nothofagus-dominated southern forests using remote sensing time series analysis. J. Appl. Entomol. 143, 787–796.
Fajardo, A., Gazol, A., Mayr, C., Camarero, J.J., 2019. Recent decadal drought reverts warming-triggered growth enhancement in contrasting climates in the southern Andes tree line. J. Biogeogr. 6, 1367–1379.
Fritts, H.C., 1976. Tree Rings and Climate. Academic Press, London.
Fritts, H.C., Vaganov, E.A., Sviderskaya, I.V., Shashkin, A.V., 1991. Climatic variation and tree-ring structure in conifers: empirical and mechanistic models of tree-ring width, number of cells, cell size, cell-wall thickness and wood density. Clim. Res. 97-116.
Gajardo, R., 2001. Antecedentes sobre el "roble de Santiago" o "roble blanco" (*Nothofagus macrocarpa*) y sus problemas de conservación. Rev. Bosque Nativ. 28, 3–7.
Garreaud, R., Alvarez-Garreton, C., Barichivich, J., Boisier, J.P., Christie, D., Galleguillos, M., LeQuesne, C., McPhee, J., Zambrano, M., 2017. The 2010-2015 mega drought in Central Chile: Impacts on regional hydroclimate and vegetation. Hydrol. Earth Syst. Sci. 21, 6307–6327.
Garreaud, R.D., Boisier, J.P., Rondanelli, R., Montecinos, A., Sepúlveda, H.H., Veloso-Aguila, D., 2020. The Central Chile mega drought (2010–2018): a climate dynamics perspective. Int. J. Climatol. 40 (1), 421–439.
Gea-Izquierdo, G., Nicault, A., Battipaglia, G., Dorado-Liñán, I., Gutiérrez, E., Ribas, M., Guiot, J., 2017. Risky future for Mediterranean forests unless they undergo extreme carbon fertilization. Glob. Chang. Biol. 23, 2915–2927.
Giorgi, F., Lionello, P., 2008. Climate change projections for the Mediterranean region. Glob. Planet. Chang. 63, 90–104.
González, M.E., Gómez-González, S., Lara, A., Garreaud, R., Díaz-Hormazábal, I., 2018. The 2010–2015 megadrought and its influence on the fire regime in central and south-central Chile. Ecosphere 9, e02300.
González-Reyes, Á., McPhee, J., Christie, D.A., Le Quesne, C., Szejner, P., Masiokas, M. H., Villalba, R., Muñoz, A.A., Crespo, S., 2017. Spatiotemporal variations in hydroclimate across the Mediterranean Andes (30-37 S) since the early twentieth century. J. Hydrometeorol. 18, 1929–1942.
Grissino-Mayer, H.D., 2001. Evaluating crossdating accuracy: a manual and tutorial for the computer program COFECHA. Tree-Ring Res. 57, 205–221.
Guerrieri, R., Belmecheri, S., Ollinger, S.V., Asbjornsen, H., Jennings, K., Xiao, J., Clark, K., 2019. Disentangling the role of photosynthesis and stomatal conductance on rising forest water-use efficiency. Proc. Natl. Acad. Sci. 116, 16909–16914.
Guiot, J., Boucher, E., Gea-Izquierdo, G., 2014. Process models and model-data fusion in dendroecology. Front. Ecol. Evol. 2, 52.
Gutierrez, A.G., Barbosa, O., Christie, D.A., DEL-VAL, E.K., Ewing, H.A., Jones, C.G., Marquet, P.A., Weathers, K.C., Armesto, J.J., 2008. Regeneration patterns and persistence of the fog-dependent Fray Jorge forest in semiarid Chile during the past two centuries. Glob. Chang. Biol. 14, 161–176.
Hadad, M.A., Molina, J.A., Roig Juñent, F.A., Amoroso, M.M., Müller, G., Araneo, D., Tardif, J.C., 2019. Frost record in tree rings linked to atmospheric circulation in northern Patagonia. Palaeogeogr. Palaeoclimatol. Palaeoecol. 524, 201–211.
Harris, I., Osborn, T.J., Jones, P., Lister, D., 2020. Version 4 of the CRU TS monthly high-resolution gridded multivariate climate dataset. Scientific Data. 7 (1), 1–18.
Hayhoe, K., Cayan, D., Field, C.B., Frumhoff, P.C., Maurer, E.P., Miller, N.L., Moser, S.C., Schneider, S.H., Cahill, K.N., Cleland, E.E., 2004. Emissions pathways, climate change, and impacts on California. Proc. Natl. Acad. Sci. 101, 12422–12427.
Holmes, R.L., Adams, R.K., Fritts, H.C., 1986. Tree-Ring Chronologies of Western North America: California, Eastern Oregon and Northern Great Basin with Procedures Used in the Chronology Development Work Including Users Manuals for Computer Programs COFECHA and ARSTAN.
Jones, P.D., Osborn, T.J., Briffa, K.R., 2001. The evolution of climate over the last millennium. Science 292, 662–667.
Jump, A.S., Mátyás, C., Peñuelas, J., 2009. The altitude-for-latitude disparity in the range retractions of woody species. Trends Ecol. Evol. 24, 694–701.
Keenan, T.F., Hollinger, D.Y., Bohrer, G., Dragoni, D., Munger, J.W., Schmid, H.P., Richardson, A.D., 2013. Increase in forest water-use efficiency as atmospheric carbon dioxide concentrations rise. Nature 499, 324–327.
Körner, C., Paulsen, J., 2004. A world-wide study of high altitude treeline temperatures. J. Biogeogr. 31, 713–732.
Lavergne, A., Daux, V., Villalba, R., Barichivich, J., 2015. Temporal changes in climatic limitation of tree-growth at upper treeline forests: Contrasted responses along the west-to-east humidity gradient in Northern Patagonia. Dendrochronologia 36, 49–59.

Le Quesne, C., Stahle, D.W., Cleaveland, M.K., Therrell, M.D., Aravena, J.C., Barichivich, J., 2006. Ancient *Austrocedrus* tree-ring chronologies used to reconstruct Central Chile precipitation variability from AD 1200 to 2000. J. Clim. 19, 5731–5744.

Le Quesne, C., Acuña, C., Boninsegna, J.A., Rivera, A., Barichivich, J., 2009. Long-term glacier variations in the Central Andes of Argentina and Chile, inferred from historical records and tree-ring reconstructed precipitation. Palaeogeogr. Palaeoclimatol. Palaeoecol. 281, 334–344.

Lévesque, M., Siegwolf, R., Saurer, M., Eilmann, B., Rigling, A., 2014. Increased water-use efficiency does not lead to enhanced tree growth under xeric and mesic conditions. New Phytologist. 203 (1), 94–109.

Luebert, F., Pliscoff, P., 2006. *Sinopsis Bioclimática y Vegetacional de Chile* [in Spanish]. (Editorial Universitaria, 2006).

Masiokas, M.H., Villalba, R., Luckman, B.H., Le Quesne, C., Aravena, J.C., 2006. Snowpack variations in the central Andes of Argentina and Chile, 1951–2005: large-scale atmospheric influences and implications for water resources in the region. J. Clim. 19, 6334–6352.

Mathiasen, P., Premoli, A.C., 2016. Living on the edge: adaptive and plastic responses of the tree *Nothofagus pumilio* to a long-term transplant experiment predict rear-edge upward expansion. Oecologia 181, 607–619.

Mathiasen, P., Venegas-González, A., Fresia, P., Premoli, A.C., 2020. A relic of the past: current genetic patterns of the palaeoendemic tree *Nothofagus macrocarpa* were shaped by climatic oscillations in central Chile. Ann. Bot. 126 (5), 891–904.

Matskovsky, V., Roig, F.A., Pastur, G.M., 2019. Removal of a non-climatically induced seven-year cycle from *Nothofagus pumilio* tree-ring width chronologies from Tierra del Fuego, Argentina for their use in climate reconstructions. Dendrochronologia 57. https://doi.org/10.1016/j.dendro.2019.125610.

Miranda, A., Altamirano, A., Cayuela, L., Lara, A., González, M., 2016. Native forest loss in the Chilean biodiversity hotspot: revealing the evidence. Reg. Environ. Chang. 1-13.

Miranda, A., Lara, A., Altamirano, A., Di Bella, C., González, M.E., Camarero, J.J., 2020. Forest browning trends in response to drought in a highly threatened mediterranean landscape of South America. Ecol. Indic. 115, 106401.

Montecinos, A., Aceituno, P., 2003. Seasonality of the ENSO-related rainfall variability in Central Chile and associated circulation anomalies. J. Clim. 16, 281–296.

Muñoz, A.A., Klock-Barría, K., Alvarez-Garreton, C., Aguilera-Betti, I., González-Reyes, Á., Lastra, J.A., Quesne, C.L., 2020. Water crisis in Petorca basin, Chile: The Combined effects of a mega-drought and water management. Water 12 (3), 648.

Myers, N., Mittermeier, R.A., Mittermeier, C.G., da Fonseca, G.A.B., Kent, J., 2000. Biodiversity hotspots for conservation priorities. Nature 403, 853–858. https://doi.org/10.1038/35002501.

Oliveira, J.M., Roig, F.A., Pillar, V.D., 2010. Climatic signals in tree-rings of *Araucaria angustifolia* in the southern Brazilian highlands. Austral Ecol. 35, 134–147. https://doi.org/10.1111/j.1442-9993.2009.02018.x.

O'Neill, B.C., Oppenheimer, M., Warren, R., Hallegatte, S., Kopp, R.E., Pörtner, H.O., Scholes, R., Birkmann, J., Foden, W., Licker, R., 2017. IPCC reasons for concern regarding climate change risks. Nat. Clim. Chang. 7, 28.

Pachauri, R.K., Allen, M.R., Barros, V.R., Broome, J., Cramer, W., Christ, R., Church, J.A., Clarke, L., Dahe, Q., Dasgupta, P., 2014. Climate change 2014: synthesis report. In: Contribution of Working Groups I, II and III to the Fifth Assessment Report of the Intergovernmental Panel on Climate Change.

Paritsis, J., Veblen, T.T., 2011. Dendroecological analysis of defoliator outbreaks on Nothofagus pumilio and their relation to climate variability in the Patagonian Andes. Glob. Chang. Biol. 17, 239–253.

Penuelas, J., Ogaya, R., Boada, M., Jump, S., A., 2007. Migration, invasion and decline: changes in recruitment and forest structure in a warming-linked shift of European beech forest in Catalonia (NE Spain). Ecography 30, 829–837.

Pompa-García, M., Sánchez-Salguero, R., Camarero, J.J., 2017. Observed and projected impacts of climate on radial growth of three endangered conifers in northern Mexico indicate high vulnerability of drought-sensitive species from mesic habitats. Dendrochronologia. 45, 145–155.

Ragettli, S., Immerzeel, W.W., Pellicciotti, F., 2016. Contrasting climate change impact on river flows from high-altitude catchments in the Himalayan and Andes Mountains. Proc. Natl. Acad. Sci. 113, 9222–9227.

Rahman, M., Islam, M., Braeuning, A., 2018. Tree radial growth is projected to decline in south Asian moist forest trees under climate change. Glob. Planet. Chang. 170, 106–119.

Rasband, W.S., 1997. Image J, 2014. US National Institutes of Health, Bethesda, Maryland, USA.

Rivera, J., Penalba, O., Villalba, R., Araneo, D., 2017. Spatio-temporal patterns of the 2010–2015 extreme hydrological drought across the Central Andes, Argentina. Water 9, 652.

Rodríguez-Catón, M., Villalba, R., Srur, A., Williams, A.P., 2019. Radial growth patterns associated with tree mortality in Nothofagus pumilio forest. Forests 10, 489.

Roig, F.A., 1992. Comparative wood anatomy of southern South American Cupressaceae. IAWA J. 13 (2), 151–162.

Roig, F.A., Siegwolf, R., Boninsegna, J.A., 2006. Stable oxygen isotopes ($\delta^{18}O$) in *Austrocedrus chilensis* tree rings reflect climate variability in northwestern Patagonia, Argentina. Int. J. Biometeorol. 51, 97–105.

Rojas-Badilla, M., Álvarez, C., Velásquez-Álvarez, G., Hadad, M., Le Quesne, C., Christie, D.A., 2017. Anomalías anatómicas en anillos de crecimiento anuales de *Austrocedrus chilensis* (D. Don) Pic.-Serm. et Bizzarri en el norte de su rango de distribución. Gayana. Botánica 74, 269–281.

Rozas, V., Le Quesne, C., Rojas-Badilla, M., González, M.E., González-Reyes, Á., 2018. Coupled human-climate signals on the fire history of upper Cachapoal Valley, Mediterranean Andes of Chile, since 1201 CE. Glob. Planet. Chang. 167, 137–147.

Sánchez-Salguero, R., Camarero, J.J., Carrer, M., Gutiérrez, E., Alla, A.Q., Andreu-Hayles, L., Hevia, A., Koutavas, A., Martínez-Sancho, E., Nola, P., 2017a. Climate extremes and predicted warming threaten Mediterranean Holocene firs forests refugia. Proc. Natl. Acad. Sci. 114, E10142–E10150.

Sánchez-Salguero, R., Camarero, J.J., Gutiérrez, E., González Rouco, F., Gazol, A., Sangüesa-Barreda, G., Seftigen, K., 2017b. Assessing forest vulnerability to climate warming using a process-based model of tree growth: Bad prospects for rear-edges. Glob. Chang. Biol. 23, 2705–2719.

Schlegel, F., 1962. Hallazgo de un bosque de cipreses cordilleranos en la provincia de Aconcagua. Bol. Univ. Chile 32, 43–46.

Schulman, E., 1956. Dendroclimatic Changes in Semiarid America. Dendroclimatic Changes in Semiarid America, 142 pp.

Seager, R., Osborn, T.J., Kushnir, Y., Simpson, I.R., Nakamura, J., Liu, H., 2019. Climate variability and change of Mediterranean-type climates. J. Clim. 32 (10), 2887–2915.

Smerdon, J.E., Cook, B.I., Cook, E.R., Seager, R., 2015. Bridging past and future climate across paleoclimatic reconstructions, observations, and models: a hydroclimate case study. J. Clim. 28, 3212–3231.

Solman, S.A., Sanchez, E., Samuelsson, P., da Rocha, R.P., Li, L., Marengo, J., Le Treut, H., 2013. Evaluation of an ensemble of regional climate model simulations over South America driven by the ERA-Interim reanalysis: model performance and uncertainties. Clim. Dyn. 41, 1139–1157.

Souto, C., Gardner, M., 2013. Austrocedrus chilensis. In: The IUCN Red List of Threatened Species 2013: e.T31359A2805519.

Taylor, K.E., Stouffer, R.J., Meehl, G.A., 2012. An overview of CMIP5 and the experiment design. Bull. Am. Meteorol. Soc. 93, 485–498.

Tognetti, R., Lombardi, F., Lasserre, B., Cherubini, P., Marchetti, M., 2014. Tree-ring stable isotopes reveal twentieth-century increases in water-use efficiency of *Fagus sylvatica* and *Nothofagus* spp. in Italian and Chilean mountains. PLoS One 9, 1–16.

Tolwinski-Ward, S.E., Evans, M.N., Hughes, M.K., Anchukaitis, K.J., 2011. An efficient forward model of the climate controls on interannual variation in tree-ring width. Clim. Dyn. 36, 2419–2439.

Tolwinski-Ward, S.E., Anchukaitis, K.J., Evans, M.N., 2013. Bayesian parameter estimation and interpretation for an intermediate model of tree-ring width. Clim. Past 9, 1481–1493.

Urrutia-Jalabert, R., González, M.E., González-Reyes, Á., Lara, A., Garreaud, R., 2018. Climate variability and forest fires in central and south-central Chile. Ecosphere 9, e02171.

Vaganov, E.A., Hughes, M.K., Shashkin, A.V., 2006. Growth Dynamics of Conifer Tree Rings: Images of Past and Future Environments. Springer Science & Business Media, Berlin Heidelberg.

Vaganov, E.A., Anchukaitis, K.J., Evans, M.N., 2011. How Well Understood Are the Processes that Create Dendroclimatic Records? A Mechanistic Model of the Climatic Control on Conifer Tree-Ring Growth Dynamics, in: Dendroclimatology. Springer, Dordrecht, pp. 37–75.

Van Vuuren, D.P., Edmonds, J., Kainuma, M., Riahi, K., Thomson, A., Hibbard, K., Masui, T., 2011. The representative concentration pathways: an overview. Climat. Change. 109 (1–2), 5.

Venegas-González, A., Roig, F.A., Gutiérrez, A.G., Peña-Rojas, K., Tomazello Filho, M., 2018a. Efecto de la variabilidad climática sobre los patrones de crecimiento y establecimiento de *Nothofagus macrocarpa* en Chile central. Bosque 39, 81–93.

Venegas-González, A., Roig, F.A., Gutiérrez, A.G., Tomazello Filho, M., 2018b. Recent radial growth decline in response to increased drought conditions in the northernmost *Nothofagus* populations from South America. For. Ecol. Manag. 409, 94–104.

Venegas-González, A., Roig, F.A., Peña-Rojas, K., Hadad, M.A., Aguilera-Betti, I., Muñoz, A.A., 2019. Recent consequences of climate change have affected tree growth in distinct *Nothofagus macrocarpa* (DC.) FM Vaz & Rodr age classes in Central Chile. Forests 10, 653. https://doi.org/10.3390/f10080653.

Viale, M., Garreaud, R., 2015. Orographic effects of the subtropical and extratropical Andes on upwind precipitating clouds. J. Geophys. Res. Atmos. 120, 4962–4974.

Villagrán, C.M., 1995. Quaternary History of the Mediterranean Vegetation of Chile. Ecology and Biogeography of Mediterranean Ecosystems in Chile, California, and Australia. Springer, pp. 3–20.

Villalba, R., Veblen, T.T., 1998. Influences of large-scale climatic variability on episodic tree mortality in northern Patagonia. Ecology 79, 2624–2640.

Vuille, M., Franquist, E., Garreaud, R., Lavado Casimiro, W.S., Cáceres, B., 2015. Impact of the global warming hiatus on Andean temperature. J. Geophys. Res. Atmos. 120, 3745–3757.

Wilmking, M., van der Maaten-Theunissen, M., van der Maaten, E., Scharnweber, T., Buras, A., Biermann, C., Smiljanic, M., 2020. Global assessment of relationships between climate and tree growth. Global Change Biology 26, 3212–3220.

Zambrano, F., Lillo-Saavedra, M., Verbist, K., Lagos, O., 2016. Sixteen years of agricultural drought assessment of the BioBío region in Chile using a 250 m resolution Vegetation Condition Index (VCI). Remote Sens. 8, 530.

Zeng, X., Evans, M.N., Liu, X., Wang, W., Xu, G., Wu, G., Zhang, L., 2019. Spatial patterns of precipitation-induced moisture availability and their effects on the divergence of conifer stem growth in the western and eastern parts of China's semi-arid region. For. Ecol. Manag. 451, 117524.